THE JOURNAL OF PHYSICAL CHEMISTRY LETTERS
A JOURNAL OF THE AMERICAN CHEMICAL SOCIETY

pubs.acs.org/JPCL
Letter

eCoral: How Electrolysis Could Restore Seawater Conditions Ideal for Coral Reefs

Eric W. Lees, Christophe Tournassat, Adam Z. Weber, and Pupa U. P. A. Gilbert*,#

Cite This: J. Phys. Chem. Lett. 2024, 15, 12206−12211
Read Online

ABSTRACT: Coral reefs suffer from climate change, including long-term ocean acidification (OA) and warming and short-term bleaching, tropical storms, and pollution events, all of which are increasing in frequency and severity. It is urgent yet unclear how to intervene to save coral reefs. Reversal of the ocean pH to preindustrial levels could restore coral reefs to their preindustrial growth rates; however, strategies to reverse OA on environmentally relevant scales have not been established. Anecdotally, electrolysis seems to help coral reefs recover from acidification and short-term events, but few uncontrolled studies support such claims. Here, using two independent continuum simulation approaches (COMSOL and CrunchFlow), we show the effect of electrolysis on seawater chemistry relevant to coral reef survival and growth. We conclude that near the negative electrodes, the cathodes, seawater pH, supersaturation, and carbonate concentration all increase significantly. Electrolysis of seawater, therefore, can be used to restore preindustrial ocean conditions locally to save coral reefs, an approach termed eCoral here. We anticipate these simulation results to be the starting point for controlled experiments to test whether seawater electrolysis promotes coral reef growth and restoration, as these simulations predict.

Using seawater electrolysis to increase ocean pH to preindustrial levels is the most promising strategy to mitigate the lethal effect of climate change on coral reefs. Coral reefs suffer from climate change,[1] including long-term ocean acidification and warming, plus short-term bleaching, tropical storms, and pollution events, all of which are increasing in frequency and severity.[2] Corals that host symbiotic dinoflagellates, expel them at high temperatures, a behavior termed coral bleaching,[3] and if the temperature remains elevated for several weeks they die. Ocean acidification (OA),[4] instead, is constantly and linearly progressing since industrial times, with seawater pH decreasing from 8.2 in 1800 to 8.0 today, and predicted to reach 7.7 by 2100.[5] pH has a unique thermodynamic definition ($pH = -\log_{10}(a_{H^+})$, where a_{H^+} is the H^+ activity or free concentration, but the term "pH" has been used by various scientific communities in association with different measurement procedures and assumptions.[6] The above pH values 8.2, 8.0, and 7.7 use the most common definition in seawater geochemistry ($pH = -\log_{10}[H^+]$, where $[H^+]$ is the H^+ molal concentration.[6] Using the thermodynamic definition, the preindustrial, current, and end of century pH values are 8.4, 8.2, and 7.9, respectively. Interventions to reduce atmospheric CO_2 are being proposed,[7,8] but their effect is going to be too slow for coral reefs' survival. Directly addressing OA by increasing ocean pH could more rapidly restore coral reefs to their preindustrial growth rates[9] and thus ensure their survival.

It is urgent yet unclear how to intervene to rescue coral reefs from both OA and warming. Currently, oceans are still supersaturated with respect to aragonite ($CaCO_3$), meaning that their conditions induce net precipitation, but by 2050 they are predicted to switch to net dissolution of aragonite.[10] Organisms that form aragonite skeletons therefore may no longer be able to do so in 25 years. All corals that form a hard skeleton, termed stony or scleractinian corals, have been depositing exclusively aragonite skeletons since the mid-Triassic, 240 million years ago (Ma);[11] thus, they are not expected to survive or make skeletons in the second half of this century.[10] Coincidentally, the 7.7 pH predicted for 2100 is identical to that estimated for 240 Ma[12] when scleractinian corals first appeared, but of course we cannot expect corals to adapt in decades rather than millions of years.[13]

Bleaching events are short-lived but increasing in frequency and duration,[14] and OA is constantly worsening; thus, interventions to save corals and the entire reef ecosystems they support are urgently needed. Most interventions, thus far, include reintroduction, after bleaching events, of coral fragments,[15] which have limited success and are unfeasible on a global scale. Reversal of OA, however, enhances calcification in coral reefs and may significantly help corals

Received: September 16, 2024
Revised: November 11, 2024
Accepted: November 13, 2024
Published: December 3, 2024

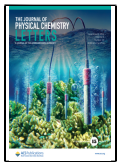

https://doi.org/10.1021/acs.jpclett.4c02715
J. Phys. Chem. Lett. 2024, 15, 12206−12211

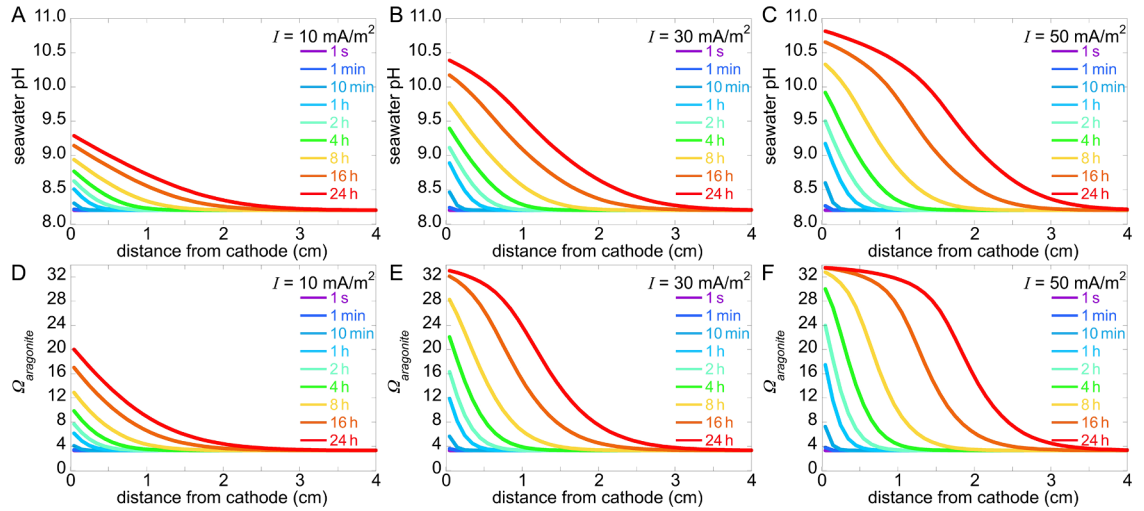

Figure 1. Simulation results of pH and supersaturation ($\Omega_{aragonite}$) at the cathode in seawater, plotted as a function of distance from the cathode, at different times (1 s to 1 day) at 3 different current densities. Simulation results were obtained using CrunchFlow at 28 °C.

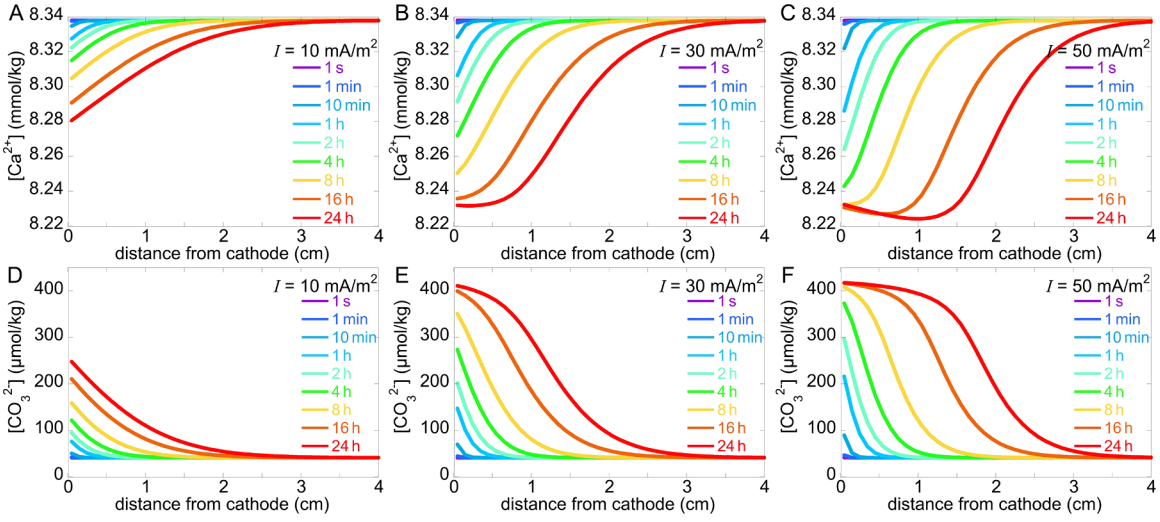

Figure 2. Simulation results of calcium and carbonate concentrations at the cathode, plotted as a function of distance from the cathode, at different times and current densities as in Figure 1. CrunchFlow results were at 28 °C.

survive both OA and bleaching events.[9] Instead of chemically reversing OA, a completely different approach involving electrical currents in metal grids (i.e., electrolysis[7]) has been used for decades,[16,17] but, surprisingly, there have not been controlled studies to quantify the effect of water electrolysis on coral reef growth, to see if corals benefit from seawater electrolysis, and, if so, why. Anecdotally, direct seawater electrolysis enhances coral growth rate, protects corals during bleaching events and during the seawater turbidity events that follow tropical storms and kill surrounding corals.[16,18] These statements, however, remain anecdotal because without control, nonelectrified grids with precisely the same corals, in the same environment, at the same time as electrified grids, a rigorous comparison is impossible. Such controlled experiments have never been done, and as a first step, it is prudent to examine and test the theoretical validity of this approach. To this end, we set out to simulate electrolysis in seawater, as previously done in other systems,[19] in order to evaluate beneficial or detrimental chemical conditions for coral growth on electrified grids.

Here, we used two independent approaches (COMSOL Multiphysics and a version of CrunchFlow that includes electrical currents[20]) to simulate the response of all relevant seawater parameters in proximity of the working negative electrodes. These simulations take into account diffusion, migration, and acid−base reactions of the 15 most abundant ionic species in seawater using a comprehensive set of activity coefficients. They also take into account convection, that is, mass transport due to ocean currents. These simulations helped understand the dynamics of the calcium and carbonate speciation in the vicinity of the two electrodes where water oxidation[19] takes place. The negatively charged electrode is the cathode, where the pH increases due to hydroxide formation and H_2 gas evolves. Corals should be installed directly on or near the cathode. The positively charged electrode is the anode, where pH decreases, Cl_2 and O_2 gases evolve in seawater[21] (as opposed to only O_2 in distilled water). The anode should be installed downstream with respect to the water currents in coral reefs. The results for pH, supersaturation with respect to aragonite ($\Omega_{aragonite}$), calcium, and carbonate concentrations by the cathode are presented in

https://doi.org/10.1021/acs.jpclett.4c02715
J. Phys. Chem. Lett. 2024, 15, 12206−12211

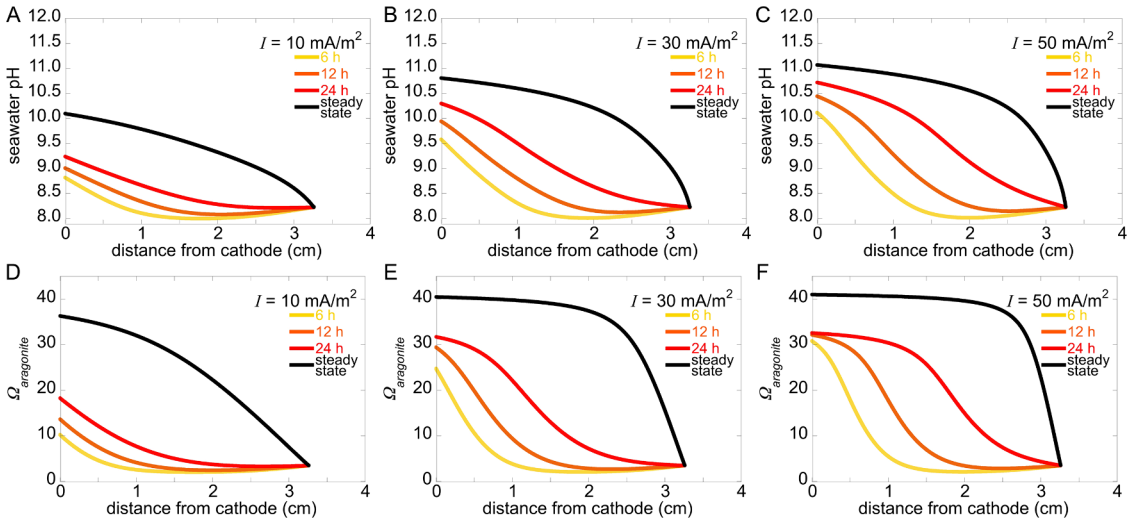

Figure 3. Simulation results for the transient and steady-state pH and supersaturation ($\Omega_{aragonite}$) near the cathode, again plotted as a function of distance from the cathode, after 6, 12, and 24 h and at steady state, which is reached after 7 days, using 3 different current densities. Simulation results obtained using COMSOL at 28 °C.

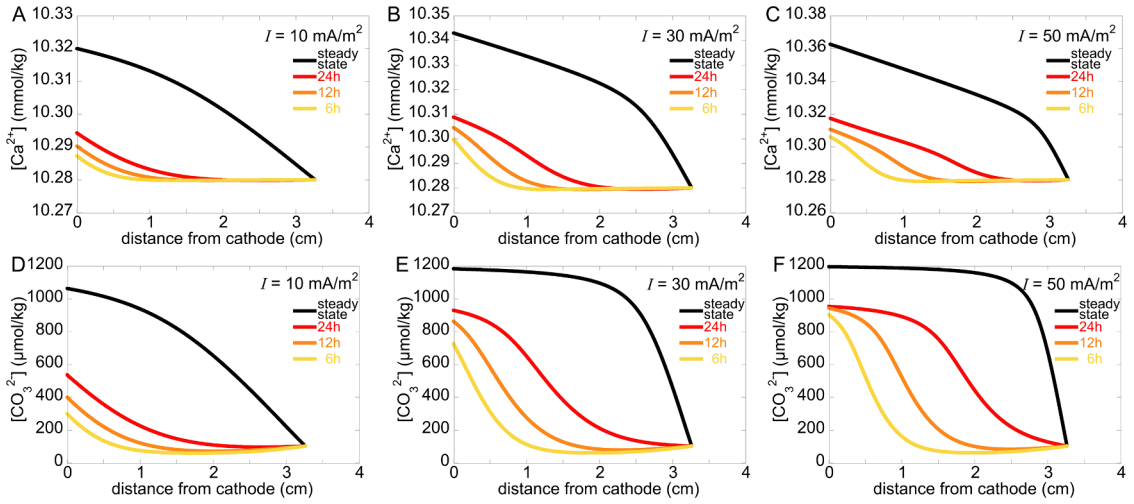

Figure 4. Simulation results for the transient and steady-state Ca and carbonate concentrations near the cathode, again plotted as a function of distance from the cathode, after 6, 12, and 24 h and at steady state, which is reached after 7 days, using 3 different current densities. Simulation results obtained using COMSOL at 28 °C.

Figures 1 and 2. The same parameters by the counter electrode, the anode, are presented in Figure S1 and S2.

Importantly, the pH used in the simulations is the thermodynamic definition, which includes the activity of protons (a_{H^+}):[6]

$$\mathrm{pH} = -\log_{10}(a_{H^+})$$

This thermodynamic definition of pH is important to use in the simulations to account for and simulate the (bi)carbonate equilibrium properly. Using the thermodynamic definition, the current seawater pH is 8.2; thus the simulations in Figure 1 and Figure S1 converge to this value at a distance of a few centimeters from the cathode and the anode, respectively.

From thermodynamics, the aragonite supersaturation ($\Omega_{aragonite}$) is defined as

$$\Omega_{aragonite} = \frac{a_{Ca^{2+}} a_{CO_3^{2-}}}{K_{sp}}$$

where K_{sp} is the solubility product of aragonite from seawater, $K_{sp} = 10^{-8.24}$.[22]

From the results in Figures 1 and 2, we conclude that, even at relatively low current densities (I = 0.01−0.05 A/m^2) the seawater conditions near the cathode are much more favorable to aragonite formation than those in bulk seawater, with much higher pH, and carbonate concentrations up to 3.3 cm from the cathode. Note that the Ca^{2+} concentration decreases only very slightly near the cathode, leading to an overall marked increase of $\Omega_{aragonite}$. The equal and opposite results at the anode are presented in Figures S1 and S2.

To understand the mass-transfer "boundary layer" between the surface of the cathode and bulk seawater with higher fidelity, COMSOL Multiphysics was used with a linear convective velocity of 1 m/s, which is representative of ocean current velocities measured by NASA.[23] In contrast to the CrunchFlow model, the COMSOL simulation uses nonequilibrium mass-action kinetics to describe the rate of buffer, diffusion, migration, and ion-complexation reactions

https://doi.org/10.1021/acs.jpclett.4c02715
J. Phys. Chem. Lett. 2024, 15, 12206−12211

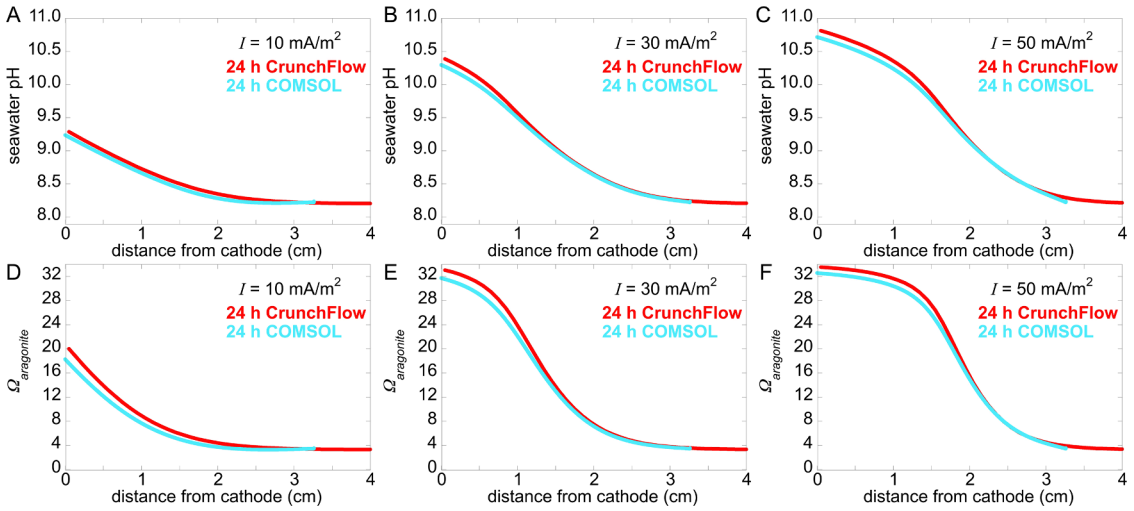

Figure 5. CrunchFlow and COMSOL simulation results compared. These are the same data already presented in Figures 1 and 3, plotted here on the same scales and panels to estimate the goodness of their agreement.

within the boundary layer. This is an important feature because near the cathode, where hydroxides are formed rapidly, the (bi)carbonate buffer reaction is known to occur out of chemical equilibrium.[24,25] The boundary-layer thickness (L_{BL}) for the COMSOL model is defined using the Churchill–Bernstein equation for cross-flow of fluid across a cylindrical geometry to account for convection,[26]

$$Sh = 0.3 + \frac{0.62Re^{1/2}Sc^{1/3}}{\left(1 + \left(\frac{0.4}{Sc}\right)^{2/3}\right)^{1/4}}\left(1 + \left(\frac{Re}{282000}\right)^{5/8}\right)^{4/5}$$

where *Sh*, *Sc*, and *Re* are the Sherwood, Schmidt, and Reynolds numbers, respectively. The boundary layer thickness was determined based on a cathode cylinder diameter of 1 cm, which is a typical diameter for the rebar electrodes used for seawater electrolysis.

$$L_{BL} = \frac{1\ \text{cm}}{Sh}$$

In this simulation, the boundary layer is where all concentrations change from the surface reaction site out to the bulk values (L_{BL} = ∼3.3 cm from the cathode).

The COMSOL simulations show in Figure 3 that the $\Omega_{aragonite}$ and pH profiles increase with an increasing current density in close proximity to the electrodes. In addition, the simulation elucidates the conditions near the cathode at steady-state, which is particularly important for understanding how coral growth will benefit from prolonged electrolysis. The results shown in Figure 3 demonstrate that the elevated $\Omega_{aragonite}$ and pH extend further into the boundary layer at steady-state than during transient operation. The corresponding Ca^{2+} and carbonate concentration profiles are shown in Figures 3 and 4. The transient simulations of 30 and 50 mA/m^2 no longer change with time after 6 days of electrolysis, indicating that a steady state is reached after 6 days (Figure S3). At 10 mA/m^2, 12 days of electrolysis are required to reach steady-state.

The COMSOL results are consistent with the CrunchFlow results for pH and $\Omega_{aragonite}$, whereas the calcium and carbonate concentrations are significantly different. The Ca concentration by the cathode decreases slightly in CrunchFlow, but it increases slightly in COMSOL. In COMSOL, Ca^{2+} ions are attracted to the negatively charged cathode and are driven there by migration. In CrunchFlow the consideration of additional aqueous complexes ($NaHCO_3$, $MgHCO_3^+$, $NaCO_3^-$, $CaHCO_3^-$, $CaCO_3$, $SrHCO_3^+$, $SrCO_3$, $CaSO_4$, $CaCl^+$, $CaCl_2$, $MgSO_4$, KSO_4^- and $MgCl^+$) as well as the update of aqueous activity coefficient with changes in water composition led to additional intricate coupling terms, which were responsible for the observed small Ca^{2+} concentration decrease. A simulation run made without the consideration of calcium aqueous complexes resulted in the prediction of an increase in Ca^{2+} concentration at the cathode (not shown). In both cases, however, the calcium concentration changes are minimal, and not relevant, because there is plenty of Ca in seawater, and [Ca] never limits calcification.

Carbonate ions, instead, increase by the cathode for both simulations but by different amounts, ∼3× more in COMSOL than in CrunchFlow. In both approaches, the carbonate concentration goes up near the cathode because the OH^- ions produced at the cathode react with dissolved bicarbonate to form carbonate. The discrepancy between the COMSOL and CrunchFlow concentration profiles is due to the ion complexation reactions considered by CrunchFlow, which cause Ca^{2+} and carbonate to be complexed with other species in solution. The COMSOL simulation considers only $MgCO_3$ complexation. Thus, COMSOL finds a greater concentration of both free Ca^{2+} and free carbonate. Most relevantly, in both simulations, the carbonate concentration increase by the cathode is significant. This is important because seawater is relatively carbonate-poor, thus increasing carbonate significantly increases aragonite's stability (i.e., its supersaturation), thus favoring higher precipitation rate, biogenically or abiotically.

The two simulation approaches are dramatically different: one assumes that all aqueous complexation reactions are at equilibrium (CrunchFlow), and the other uses the law of mass action to calculate the buffer reaction rates explicitly in the forward and reverse reaction directions (COMSOL). The COMSOL simulation, therefore, accounts for the finite nature of the forward and reverse buffer reaction rates, which can result in nonequilibrium distributions of dissolved buffering species when the rate of hydroxide generation is faster than the

https://doi.org/10.1021/acs.jpclett.4c02715
J. Phys. Chem. Lett. 2024, 15, 12206−12211

carbonate buffer reaction rates.[24] Conversely, CrunchFlow accounts (i) for the formation of a larger number of aqueous complexes, which is only limited by the information provided by the thermodynamic database, and (ii) for the changes in the activity coefficients of aqueous species in agreement with changes in water composition. Despite these significant differences, the results of the two approaches are in agreement, as demonstrated by the almost overlapping curves in Figure 5.

These results are promising because they indicate that conditions favorable for aragonite precipitation (abiotic or biogenic alike) extend 3.3 cm from the cathode surface during the continued electrolysis. These results demonstrate that corals could, in principle, benefit from electrolysis, because the pH is locally higher near the cathode, the carbonate concentration, normally very low in seawater (40 μmol/kg of seawater), is much greater (5× to 10× greater for 10 to 50 mA/m^2, respectively). The supersaturation with respect to aragonite ($\Omega_{aragonite}$) is also much higher. All three parameters contribute to making the energetic cost of calcification significantly lower, thus making it easier and/or faster for corals to build their spherulitic aragonite skeletons.[27] Moreover, the alkaline and carbonate-rich conditions enabled by electrolysis could, in principle, help corals survive stress events. Controlled experiments, to compare coral growth rates on electrified and nonelectrified grids, are therefore justifiable on the solid basis of seawater chemistry and electrolysis.

The results of two independent simulation approaches demonstrate that electrolysis effectively and locally restores seawater to preindustrial conditions. A scaling up to global proportions, by using, for example, inexpensive, movable, floating solar panels and wire electrodes is how eCoral could potentially save entire reefs. But first, experimental validation with living corals is necessary to measure if, by how much, and with which values of voltage, current, current density, and range of effectiveness corals most benefit from seawater electrolysis.

■ ASSOCIATED CONTENT

Supporting Information

The Supporting Information is available free of charge at https://pubs.acs.org/doi/10.1021/acs.jpclett.4c02715.

CrunchFlow cathode pH (XLSX)

CrunchFlow cathode Omega (XLSX)

CrunchFlow cathode Ca (XLSX)

CrunchFlow cathode CO3 (XLSX)

CrunchFlow anode Ca (XLSX)

CrunchFlow anode CO3 (XLSX)

CrunchFlow anode Omega (XLSX)

CrunchFlow anode pH (XLSX)

COMSOL cathode Ca (XLSX)

COMSOL cathode CO3 (XLSX)

COMSOL cathode Omega (XLSX)

COMSOL cathode pH (XLSX)

Experimental section including the COMSOL model development, additional figures of simulation results for pH, supersaturation, and concentrations, and tables of activity coefficients, buffer reaciton constants, diffusion coefficients, and bulk seawater concentrations (PDF)

■ AUTHOR INFORMATION

Corresponding Author

Pupa U. P. A. Gilbert − *Department of Physics, University of Wisconsin, Madison, Wisconsin 53706, United States; Departments of Chemistry, Materials Science and Engineering, and Geoscience, University of Wisconsin, Madison, Wisconsin 53706, United States; Chemical Sciences Division, Lawrence Berkeley National Laboratory, Berkeley, California 94720, United States;* orcid.org/0000-0002-0139-2099; Email: pupa@physics.wisc.edu

Authors

Eric W. Lees − *Energy Technologies Area, Lawrence Berkeley National Laboratory, Berkeley, California 94720, United States; Department of Chemical and Biological Engineering, University of British Columbia, Vancouver V6T 1Z4, Canada*

Christophe Tournassat − *Energy Geosciences Division, Lawrence Berkeley National Laboratory, Berkeley, California 94720, United States; ISTO, UMR 7327, Univ Orleans, CNRS, BRGM, OSUC, F-45071 Orléans, France;* orcid.org/0000-0003-2379-431X

Adam Z. Weber − *Energy Technologies Area, Lawrence Berkeley National Laboratory, Berkeley, California 94720, United States;* orcid.org/0000-0002-7749-1624

Complete contact information is available at: https://pubs.acs.org/10.1021/acs.jpclett.4c02715

Author Contributions

P.U.P.A.G. conceived the study, E.W.L. and C.T. did simulations and calculations. A.Z.W. discussed the results. P.U.P.A.G. wrote the manuscript, and all authors edited it.

Author Contributions

[#]Previously publishing as Gelsomina De Stasio.

Funding

P.U.P.A.G. received 40% support from the Department of Energy, Basic Energy Science, Chemical Sciences, Geosciences, Biosciences, Geosciences (DOE-BES-CSGB-Geosciences) Grant DE-FG02-07ER15899 at University of Wisconsin, 40% support from award FWP-FP00011135 also from DOE-BES-CSGB-Geosciences at Lawrence Berkeley National Laboratory under Contract no. DE-AC02-05CH11231, and 20% support from the National Science Foundation (NSF), Biomaterials Grant DMR-2220274. E.W.L acknowledges support from a Natural Science and Engineering Research Council of Canada Postdoctoral Fellowship. C.T. acknowledges the funding support by a grant overseen by the French National Research Agency (ANR) as part of the "Investissements d'Avenir" Programme LabEx VOLTAIRE, 10-LABX-0100. The numerical implementation of electrical current within CrunchFlow was developed as part of the DOE-BES-Geoscience program at LBNL, under Contract DE-AC02-05CH11231.

Notes

The authors declare no competing financial interest.

■ REFERENCES

(1) Schmidt, C. A.; Stifler, C. A.; Luffey, E. L.; Fordyce, B. I.; Ahmed, A.; Barreiro Pujol, G.; Breit, C. P.; Davison, S. S.; Klaus, C. N.; Koehler, I. J.; et al. Faster crystallization during coral skeleton formation correlates with resilience to ocean acidification. *J. Am. Chem. Soc.* **2022**, *144*, 1332−1341.

(2) Hughes, T. P.; Kerry, J. T.; Baird, A. H.; Connolly, S. R.; Dietzel, A.; Eakin, C. M.; Heron, S. F.; Hoey, A. S.; Hoogenboom, M. O.; Liu, G. Global warming transforms coral reef assemblages. *Nature* **2018**, *556* (7702), 492−496. Hoegh-Guldberg, O.; Skirving, W.; Dove, S. G.; Spady, B. L.; Norrie, A.; Geiger, E. F.; Liu, G.; De La Cour, J. L.; Manzello, D. P. Coral reefs in peril in a record-breaking year. *Science* **2023**, *382* (6676), 1238−1240.
(3) Van Hooidonk, R.; Maynard, J.; Planes, S. Temporary refugia for coral reefs in a warming world. *Nature Climate Change* **2013**, *3* (5), 508−511.
(4) Comeau, S.; Cornwall, C.; DeCarlo, T. M.; Doo, S.; Carpenter, R.; McCulloch, M. Resistance to ocean acidification in coral reef taxa is not gained by acclimatization. *Nature Climate Change* **2019**, *9* (6), 477−483.
(5) Pörtner, H.-O.; Roberts, D. C.; Masson-Delmotte, V.; Zhai, P.; Tignor, M.; Poloczanska, E.; Weyer, N. Summary for Policymakers. *The ocean and cryosphere in a changing climate: IPCC special report on the ocean and cryosphere in a changing climate*; IPCC, 2019; pp 3−35, . See page 37 for 2100 projection.
(6) Marion, G. M.; Millero, F. J.; Camões, M. F.; Spitzer, P.; Feistel, R.; Chen, C.-T. pH of seawater. *Marine Chemistry* **2011**, *126* (1−4), 89−96.
(7) Eisaman, M.; Schwartz, D.; Amic, S.; Larner, D.; Zesch, J.; Torres, F.; Littau, K. Energy-efficient electrochemical CO2 capture from the atmosphere. *Tech Procs 2009 Clean Technol. Conf and Trade Show*; TechConnect, 2009; pp 3−7.
(8) Zhang, R.; Zhang, Z.; Chen, X.; Jiang, J.; Hua, L.; Jia, X.; Bao, R.; Wang, F. Pyrogenic Carbon Degradation by Galvanic Coupling with Sprayed Seawater Microdroplets. *J. Am. Chem. Soc.* **2024**, *146* (12), 8528−8535. Cao, Z.; Kim, D.; Hong, D.; Yu, Y.; Xu, J.; Lin, S.; Wen, X.; Nichols, E. M.; Jeong, K.; Reimer, J. A. A molecular surface functionalization approach to tuning nanoparticle electrocatalysts for carbon dioxide reduction. *J. Am. Chem. Soc.* **2016**, *138* (26), 8120−8125.
(9) Albright, R.; Caldeira, L.; Hosfelt, J.; Kwiatkowski, L.; Maclaren, J. K.; Mason, B. M.; Nebuchina, Y.; Ninokawa, A.; Pongratz, J.; Ricke, K. L. Reversal of ocean acidification enhances net coral reef calcification. *Nature* **2016**, *531* (7594), 362−365.
(10) Eyre, B. D.; Cyronak, T.; Drupp, P.; De Carlo, E. H.; Sachs, J. P.; Andersson, A. J. Coral reefs will transition to net dissolving before end of century. *Science* **2018**, *359*, 908−911.
(11) Stolarski, J.; Kitahara, M. V.; Miller, D. J.; Cairns, S. D.; Mazur, M.; Meibom, A. The ancient evolutionary origins of Scleractinia revealed by azooxanthellate corals. *BMC Evol Biol.* **2011**, *11* (1), 316.
(12) Halevy, I.; Bachan, A. The geologic history of seawater pH. *Science* **2017**, *355* (6329), 1069−1071.
(13) Knoll, A. H.; Nowak, M. A. The timetable of evolution. *Sci. Adv.* **2017**, *3* (5), No. e1603076.
(14) Cornwall, W. Florida coral restoration in hot water. *Science* **2024**, *383* (6683), 576−577.
(15) Gilmour, J. P.; Smith, L. D.; Heyward, A. J.; Baird, A. H.; Pratchett, M. S. Recovery of an isolated coral reef system following severe disturbance. *Science* **2013**, *340* (6128), 69−71.
(16) Goreau, T. J. F.; Hilbertz, W. Marine ecosystem restoration: costs and benefits for coral reefs. *World Resource Rev.* **2005**, *17* (3), 375−409.
(17) Strömberg, S. M.; Lundälv, T.; Goreau, T. J. Suitability of mineral accretion as a rehabilitation method for cold-water coral reefs. *J. Experi Mar Biol. Ecol* **2010**, *395* (1−2), 153−161.
(18) Goreau, T. J. F. Marine electrolysis for building materials and environmental restoration. *Electrolysis* **2012**, *13* (InTech), 273−290. Goreau, T. J. F.; Hilbertz, W. Reef restoration using seawater electrolysis in Jamaica. *Innovative Methods of Marine Ecosystem Restoration*; CRC Press: Boca Raton, FL, 2012; pp 35−45. Goreau, T. J. F. Perspective Chapter: Electric Reefs Enhance Coral Climate Change Adaptation. In *Corals-Habitat Formers in the Anthropocene*; Chimienti, G., Ed.; IntechOpen, 2023. Goreau, T. J. F. Coral reef electrotherapy: field observations. *Front Mar Sci.* **2022**, *9*, 805113.
(19) Rolle, M.; Muniruzzaman, M.; Haberer, C. M.; Grathwohl, P. Coulombic effects in advection-dominated transport of electrolytes in porous media: Multicomponent ionic dispersion. *Geochim. Cosmochim. Acta* **2013**, *120*, 195−205.
(20) Steefel, C. I.; Appelo, C. A. J.; Arora, B.; Jacques, D.; Kalbacher, T.; Kolditz, O.; Lagneau, V.; Lichtner, P.; Mayer, K. U.; Meeussen, J. Reactive transport codes for subsurface environmental simulation. *Comp Geosci* **2015**, *19*, 445−478. Tournassat, C.; Steefel, C. I. Reactive transport modeling of coupled processes in nanoporous media. *Revs Mineral Geochem* **2019**, *85* (1), 75−109.
(21) Dresp, S. r.; Dionigi, F.; Klingenhof, M.; Strasser, P. Direct electrolytic splitting of seawater: opportunities and challenges. *ACS Energy Letters* **2019**, *4* (4), 933−942.
(22) Giffaut, E.; Grivé, M.; Blanc, P.; Vieillard, P.; Colàs, E.; Gailhanou, H.; Gaboreau, S.; Marty, N.; Made, B.; Duro, L. Andra thermodynamic database for performance assessment: ThermoChimie. *Appl. Geochem.* **2014**, *49*, 225−236. Parkhurst, D. L.; Appelo, C. *Description of input and examples for PHREEQC version 3: a computer program for speciation, batch-reaction, one-dimensional transport, and inverse geochemical calculations*; Techniques and Methods 6-A43; US Geol Survey, 2013; p 497; DOI: 10.3133/tm6A43.
(23) Shirah, G. M. H.; Dohan, K.; Lagerloef, G.; Johnson, Leann. *OSCAR Ocean Currents with Velocity*; NASA, 2012.
(24) Hashiba, H.; Weng, L.-C.; Chen, Y.; Sato, H. K.; Yotsuhashi, S.; Xiang, C.; Weber, A. Z. Effects of Electrolyte Buffer Capacity on Surface Reactant Species and the Reaction Rate of CO2 in Electrochemical CO2 Reduction. *H Phys. Chem. C* **2018**, *122* (7), 3719−3726.
(25) Bui, J. C.; Lucas, É.; Lees, E. W.; Liu, A. K.; Atwater, H. A.; Xiang, C.; Bell, A. T.; Weber, A. Z. Analysis of bipolar membranes for electrochemical CO2 capture from air and oceanwater. *Energy Environ. Sci.* **2023**, *16* (11), 5076−5095.
(26) Churchill, S. W.; Bernstein, M. A Correlating Equation for Forced Convection From Gases and Liquids to a Circular Cylinder in Crossflow. *J. Heat Transfer* **1977**, *99* (2), 300−306.
(27) (a) De Stasio, G.; Capozi, M.; Lorusso, G. F.; Baudat, P. A.; Droubay, T. C.; Perfetti, P.; Margaritondo, G.; Tonner, B. P. MEPHISTO: Performance tests of a novel synchrotron imaging photoelectron spectromicroscope. *Rev Sci Instrum* **1998**, *69* (5), 2062−2066. (b) De Stasio, G.; Perfetti, L.; Gilbert, B.; Fauchoux, O.; Capozi, M.; Perfetti, P.; Margaritondo, G.; Tonner, B. P. MEPHISTO spectromicroscope reaches 20 nm lateral resolution. *Rev Sci Instrum* **1999**, *70* (3), 1740−1742. (c) Sun, C.-Y.; Marcus, M. A.; Frazier, M. J.; Giuffre, A. J.; Mass, T.; Gilbert, P. U. P. A. Spherulitic growth of coral skeletons and synthetic aragonite: Nature's three-dimensional printing. *ACS Nano* **2017**, *11*, 6612−6622. (d) Sun, C.-Y.; Stifler, C. A.; Chopdekar, R. V.; Schmidt, C. A.; Parida, G.; Schoeppler, V.; Fordyce, B. I.; Brau, J. H.; Mass, T.; Tambutté, S.; et al. From particle attachment to space-filling coral skeletons. *Procs Natl. Acad. Sci.* **2020**, *117* (48), 30159−30170.

https://doi.org/10.1021/acs.jpclett.4c02715
J. Phys. Chem. Lett. 2024, 15, 12206−12211